THE HIRENASD ELASTIC WING MODEL AND AEROELASTIC TEST PROGRAM IN THE EUROPEAN TRANSONIC WINDTUNNEL (ETW)

J. Ballmann
Department of Mechanics (LFM), RWTH Aachen University
D – 52056 Aachen, Germany
Co-authors: A. Dafnis, ILB, K.-H. Brakhage, IGPM, C. Braun, LFM, M. Kämpchen, ILB, H. Korsch, ILB, H.-G. Reimerdes, ILB, H. Olivier, SWL, all RWTH Aachen University

SURVEY

The paper presents an overview of the experimental high Reynolds number aerostructural dynamics (HIRENASD) project which is prepared by RWTH Aachen University. Experiments will be performed with an elastic wing model under cryogenic conditions at transonic Mach numbers and Reynolds numbers up to 70 millions in ETW in 2006.

1. INTRODUCTION

Only very few aeroelastic windtunnel experiments with oscillating elastic wings in the transonic flow regime and at flight Reynolds numbers of large transport aircrafts have been performed so far [1], even though the transonic regime is characterised by strong nonlinearities with shocks and phenomena which strongly depend on the Reynolds number such as shock-induced steady and unsteady flow separation, and possible shock-buffeting with unsteady fluid-structure interaction. Besides the necessity of a thorough understanding of the aeroelastic phenomena, windtunnel experiments with elastic wings at Mach and Reynolds numbers of real transport aircrafts are needed for the validation of methods for computational aeroelasticity (CAE). Under cryogenic conditions it is possible to achieve Reynolds numbers of up to 80 million in ETW at high transonic Mach numbers, similar to the conditions of high capacity aircrafts in cruise flight. A further advantange of ETW is that the parameters Mach number, Reynolds number, and dynamic pressure, which are influencing the areoelastic behaviour of the wing, can be varied independently. For a more detailed description and comparison of the flow parameter range see Fig. 1. Full and half-model testing are possible in ETW.

With funding by the Deutsche Forschungs-gemeinschaft (DFG), the collaborative research center "Flow Modulation and Fluid-Structure Interaction at Airplane Wings" (SFB 401) at RWTH Aachen University is preparing aeroelastic experiments, which will be performed in the European Transonic Windtunnel (ETW), engaging DLR concerning aeroelastic data acquisition and getting support from Airbus for development and construction of a 6-components piezo balance for dynamic force measurements in ETW.

The experiments will be performed with an elastic pure wing model which will be mounted on a 6-components piezo balance in the windtunnel ceiling similar as for half-model testing [2] and will include steady and unsteady measurements. The windtunnel model corresponds to the SFB 401 clean wing reference configuration [3], which has the profile BAC 3-11 reported in AGARD-AR-303 [4], arranged for cruise flight, and a planform typical for a wing of high speed transport aircrafts.

In different sub-projects of SFB 401, the elastic windtunnel model has been designed to meet required aeroelastic properties in consideration of the multidisciplinary aspects. The dynamic dimensioning mainly focusses on clearly separated eigenshapes and eigenfrequencies, which can be influenced by the application of additional masses. The design process has been iterative. In each design step the structural properties of the wing model have been computed applying computational structural dynamic (CSD) methods, while a Navier-Stokes solver was used to compute the aerodynamic loads. An aeroelastic solver, which fully couples the solid-fluid interaction (SOFIA) has been developed and validated within the frame of SFB 401 [5], [6], [7], [8], [9], [10], [11], is applied to predict the steady and unsteady aeroelastic behaviour of the model under windtunnel flow conditions.

In the paper, the general approach during the model design and qualification will be described and the testing program including first predictions using the CAE package SOFIA will be presented.

2. MOTIVATION FOR THE PROJECT

One motivation for the project is to improve the physical knowledge about aerostructural dynamics phenomena in the transonic regime and to gather experimental aeroelastic data for numerical code validation in a wide range of Reynolds numbers and aerodynamic loading. First, aerodynamic polars will be measured in steady flow under different dynamic pressure, Reynolds number and Mach number conditions in the windtunnel, including deformation measurement of the respected aeroelastic

equilibrium configurations of the wing model. Thereafter, aerostructural dynamic processes will be considered in forced and free vibrations to study aerodynamic damping mechanisms, aerostructural coupling in presence of unsteady shock/boundary-layer interaction, and unsteady flow separation up to buffeting onset.

The data will be gathered in a freely accessible data base to make it available to the aeroelastic research community and to promote the transonic aeroelastic research in universities, providing an advanced data basis for modelling enhancement, and validation of CAE methods and aerodynamic codes as well.

3. ELASTIC MODEL DESIGN

3.1. Wing model geometry and material

The planform of the wing model has the typical characteristics of a wing for a large transport aircraft. In its 1st design it corresponds to the SFB 401 reference configuration [3]. The leading edge sweep angle is 34°, the span of the scaled model is 1285.71 mm and the chord decreases from its root value in three sections piecewise linearly to the tip value. Fig. 2 shows the chord length values at the three wing-section transitions which varied in the first design phase from 525.71 mm at the wing root to 142.86 mm at the wing tip.

The chosen profile corresponds to the BAC 3-11/RES/30/21 cruise flight profile which is supercritical and has 11 % thickness [3]. Only in the first wing section from the root the profile thickness was modified such that it varies linearly from 15 % at the root to 11 % at the transition to the second section. The increment of the profile thickness is completely restricted to the first section on the lower wing surface. Only there the profile deviates from the BAC 3-11 airfoil, see bottom of Fig. 3.

In order to realise the highest Reynolds numbers, the flow medium nitrogen has to be cooled down to about 120 K and the windtunnel total pressure has to be rised to about 400 kPa, resulting in a dynamic pressure of up to 130 kPa at transonic Mach numbers. Therefore a highly tenacious steel is needed as model material which preserves adequately its material data over the full range of flow temperatures from cryogenic to environmental temperatures to endure dynamic loading under the respective conditions. The material of choice is a C200 Maraging steel (G90c) with 18° Nickel [12], [13]. Two forged blocks of the material were used to mill the two parts of which the elastic wing model is composed.

3.2. Aeroelastic model design

Computer aided geometrical design (CAGD) tools [14] have been used for the design of the outer surface of the model and converted to CAD data applying the CATIA software. In order to check the CAD data, a 1:1 scaled pre-model has been first milled out of a block of the solid foam material NECURON (see photograph in Fig. 3).

The SOFIA software has been applied to compute the design loads. Fig. 4 shows the lift over angle of attack and the displacement at wing tip for the flow parameters Mach number Ma=0.9, Reynolds number Re=70 millions and dynamic pressure q_∞=122 kPa. For this 1st design case the model was assumed as a massive solid. The real model is less stiff because it is hollowed out to provide place for the measurement instrumentation. The turbulence model applied for finding the dimensioning design loads was Baldwin-Lomax (BL). For the design point, the lift calculated using the BL-model was 17 kN and the wing tip displacement 5.4 cm. For the hollowed wing the flow conditions chosen for the design point, with angle of attack α=3° resulted in the pressure distribution presented in Fig. 5 for the deformed wing in static equilibrium. Cp distribution is plotted in four span wise cross sections. This result was produced using Spalart-Allmaras turbulence modelling.

3.3. Model design modification

The 1st design was based on the intention of only clean wing aeroelastic experiments. During the manufacturing process of the pre-model, possible tip devices came into discussion and, finally, it has been decided to modify stiffness and strength of the model such that for a second test series the attachment of a winglet can be provided without changing the span (see Fig. 6). For that case higher aerodynamic loads are to be expected which were responsible for the enlargement of the cross section in the final design of the clean wing model. Its geometry is presented in Fig. 7. The planform shows now a root chord of 549.37 mm and a tip chord of 149.29 mm. Half span and relative thickness distribution of the profile remained unchanged.

As already mentioned above, the model consists of two pieces, the upper and the lower part which have a jointing surface with straight separation line along the jointing leading ledge and a meandering separation line on the bottom surface of the model, as can be seen on the bottom side view of the wing model in Fig. 7. To impede relative motion of the model parts, a growed and tongued joint concept has been applied in span- and cross-direction along the jointing surface. This can be seen in Fig. 8. This figure shows the interior of the top and the bottom parts of the wing model, where one can recognise seven ribs for implementation of pressure sensors and three stringers in longitudinal direction, of which the central ends at about 60 % span. The final element code MARC/MENTAT has been used to compute eigenshapes and eigenfrequencies for a volume discretisation of the model in its final design.

The first two modes are bending dominated, the third mode belongs to inplane motion, the fourth mode is still bending dominated, the fifth is torsion dominated, as can be seen in Fig. 9, where the red/ dotted line indicates the undeformed wing. The modes and frequencies registered in the figure were calculated assuming the model to be fixed in the root section.

To test the chosen contact surface concept with notches and teeth, a smaller two-piece pre-model has been designed (see Fig. 10), manufactured and tested (see Fig. 11) with respect to high cycle fatigue, fracture toughness of the mounting bolts and influence of dry friction contact phenomena, e.g. stick slip motion. There was no negative effect observed, the pre-model behaved like a one-piece model. The jointing surface design for the wing model was accepted, and checking of the CAD machining data was performed as for the outer surface by testwise milling of the interior surface from a block of the foam material NECURON (see Fig. 12 right top). Having excluded all CAD-data errors, the machining of the wing model inner and outer surface was carried out. Fig. 12 and Fig. 13 show the two metal wing model parts from the inner and outer side on photographs. The outer side has been polished before implementing the pressure holes by an erosion technique.

The complete windtunnel assembly consists of a new windtunnel balance, which is connected with a containment including the wing clamping and hosting the vibration excitation mechanism. In order to alleviate the influence of the ceiling boundary layer of the windtunnel, a fuselage substitute is provided around the wing. It will be fixed to a mounting plate at the turntable on the tunnel ceiling and will have no mechanical contact with the elastic wing model (see Fig. 14). A round arch labyrinth sealing is implemented on the fuselage substitute side about the wing root.

4. VIBRATION EXCITATION

Forced vibration of the windtunnel model will be realised by two dynamic force couples made up by four spanwise directed forces which are applied at respective prominent noses at the wing root side. The forces are produced by four pre-stressed piezo-stacks, mounted in a containment which is very stiff and forms one piece with the wing clamping. Therefore these forces are interior forces, acting within the assembly composed of the wing and the vibration excitation mechanism. Fig. 15 shows a zoom of the excitation mechanism and the windtunnel balance which are thermally conditioned and separated to the cold part of the windtunnel by the windtunnel wall. The excitation forces are transmitted by stacks made from the same material as the wing model, i.e. from the above mentioned maraging steel. For reasons of thermal extension the excitation mechanism containment is also made from this material. A cross-cut through the vibration excitation mechanism is sketched in Fig. 16, where one can see the fixing of the wing by bolts, the piezo-stacks for excitation, and in the background the broken circles which represent the four piezo elements of the balance. The vibration excitation concept has been tested successfully with a pre-model. Fig. 17 shows this test in the laboratory.

5. MEASURING EQUIPMENT

5.1. 6-components piezo windtunnel balance

As already mentioned, the measuring devices are four piezo-electric load cells. These are pre-stressed with 300 kN and provided for measuring forces of $\pm$ 60 kN in the cross plane and $\pm$ 100 kN in the axial direction. This balance has been designed, manufactured and assembled for the HIRENASD project. Fig. 18 shows a photograph of the balance together with the appertaining electronic devices, and Fig. 19 presents an inside view of the piezo windtunnel balance.

The new balance is a necessary measuring tool for the aeroelastic experiments with dynamic loads, because the present windtunnel balance in ETW is by far not stiff enough for dynamic measurements. Therefore, the new balance has been designed very stiff. Its lowest eigenmodes are in the range of 1000 Hz as can be read in Fig. 20, where the first two eigenshapes are plotted. For the complete windtunnel balance and model assembly the first eigenmode dropped from 31.12 Hz for the wing fixed at its root to a value of 27.32 Hz for the completely elastified assembly. For the second mode the respective value of 107.8 Hz decreased to 85.77 Hz (see Fig. 21).

5.2. Sensor equipment of the wing model

The model will be equipped with 259 cryogenic miniature/ultraminiature pressure sensors (Kulites) which are distributed in 7 cross-sections of the model. The relative span positions η of these 7 cross-sections and the respective numbers of sensors are (see also Fig. 22) as follows:

section	1	2	3	4	5	6	7
η	0.14	0.32	0.46	0.59	0.66	0.80	0.95
number	43	41	40	38	35	31	31

Because of place requirement for the sensors in the interior of the wing, the sensors and pressure holes on the bottom side of the wing model are about 2 mm shifted towards the tip, relative to the pressure holes on the model top side.

The pressure sensors have been tested under cryogenic conditions in the windtunnel KRG of DLR Göttingen. For this test an airfoil with the reference profile BAC 3-11 was manufactured from the same cryogenic steel as chosen for the ETW wing model. The airfoil chord length was 150 mm and its span 400 mm. It was instrumented with 41 Kulite pressure sensors along the middle cross-section. Fig. 23 and Fig. 24 show some time histories of signals of pressure sensors during experiments and, in the middle, the arrangement of the sensors and pressure holes along the cross-section. The signals of the sensors were selected to show measured pressure data over the period of one experiment. The middle part with mean-pressure plateau corresponds to the measuring time. Before that time one can see the establishment of the flow and after the plateau the slow down of the flow. In the two experiments selected for this paper, buffet has been observed. The flow conditions are in both cases the same for Mach number Ma=0.75 and angle of attack α=4°, but with different Reynolds numbers, namely Re=4.85 millions (stagnation temperature 262.5 K) for experiment No. 60 (Fig. 23) and Re=16.18 millions (stagnation temperature 148.5 K) for experiment No. 179 (Fig. 24). Like in the series of experiments reported in [15], experiment No. 179 was performed under cryogenic conditions. The buffet frequencies observed were 128 Hz in the lower Reynolds number case and 88 Hz in the higher Reynolds number case. Fig. 25 shows for both experiments the upper most and the down most positions of the shock during buffet. The aptitude of the pressure sensors and their implementation using special shoes was proven successfully. After the experiments all sensors could be recovered without damage.

Additionally to the pressure sensors, the windtunnel model assembly will be equipped with 17 accelerometers and 28 strain gauges, distributed in the wing model and in the excitation mechanism.

Beyond this, high speed video imaging will be employed for 3D-stereo tracking of an arrangement of markers, which are implemented on the bottom surface of the wing model. Ultra-high speed frame grabbing will allow image recording of the deformation history of the wing during vibration.

6. AEROELASTIC EXPERIMENTAL CONDITIONS IN ETW

The range of the stationary experimental conditions will contain root angles of attack in the interval $-2° < \alpha < 5°$, Mach numbers 0.8, 0.85 and 0.88, 4 levels of dynamic pressure from 38 kPa to 125 kPa and 5 levels of Reynolds numbers from $9 \cdot 10^6$ to $73 \cdot 10^6$, based on the aerodynamic mean chord amc=0.3445 m. The test envelope for Ma=0.85 is shown in Fig. 26. The aeroelastodynamic experiments are planned with forced vibration by exciting the first three bending dominated modes in hover and the first torsion dominated mode, and free vibration to evaluate the damping mechanism. The parameters Mach number, dynamic pressure and Reynolds number will be the same as for the stationary experiments. Only 2 or 3 angles of attack, including the zero lift angle of attack, are planned for the dynamic experiments.

The experiments will take place in August/ September 2006. Before that, we will be simulating a part of the test conditions in advance using the SOFIA code. One preliminary blind test result for the 1st design of the HIRENASD model is presented in Fig. 27, which shows in the left diagram the change of lift over angle of attack for the steady flow case. The diagram shows that the lift of the deformed wing in its aeroelastic equilibrium configuration has a lower value than the lift of the wing in its undeformed (jig) shape.

The right diagram of Fig. 27 exhibits the deformation motion of the wing, starting from the equilibrium configuration of the elastic wing under the aerodynamic loading of the chosen stationary flow conditions Ma=0.76, α=0°, Re=$32.05 \cdot 10^6$ and q_∞ = 117.02 kPa, and an additional external load, after removing the external load, The vibration is represented by two wing tip deflection quantities: vertical displacement and torsion. The right diagram shows the influence of aerodynamic damping which for the chosen flow conditions is between 5 and 10 %.

7. ACKNOWLEDGEMENT AND INVITATION

The funding by Deutsche Forschungsgemeinschaft is gratefully acknowledged. The authors thank Airbus Industry for supporting the balance, The German Aerospace Center (DLR) for providing data acquisition techniques and equipment and ETW for continuous advice. The Aeroelastic Community is invited to visit the project homepage http://www.lufmech.rwth-aachen.de/HIRENASD/ to get detailed information about wing model geometry and material as well as the windtunnel conditions for the model and to produce blind test results to be included in our data base, which will successively be opened to the community.

8. LITERATURE

[1] Cole, S.R., Noll, T.E., Perry, B. III: Transonic Dynamics Tunnel Aeroelastic Testing in Support of Aircraft Development. Journal of Aircraft, Vol. 40, No. 5, 2003

[2] Wright, M.C.N.: Half Model Testing at ETW. Technical Memorandum ETW/TM/2000028, Köln 2000

[3] Özger, E., Schell, I., Jacob, D.: On the Structure and Attenuation of an Aircraft Wake. AIAA

Journal of Aircraft, Vol. 38, No. 5, pp. 878-887, 2001

[4] Moir, I.-R.M. Measurements on a two-dimensional aerofoil with high-lift devices. AGARD-AR-303, Vol. II, 58-59, 1994

[5] Ballmann J. (Ed.): Flow Modulation and Fluid-Structure-Interaction at Airplane wings. Notes On Numerical Fluid Mechanics And Multidisciplinary Design, Vol. 84, pp. 105-122, 2003

[6] Ballmann, J., Boucke, A., Braun, C.: Aeroelastic Sensitivity in the Transonic Regime. Sobieczky (Ed.): Proceedings of the IUTAM Symposium Transsonicum IV, Göttingen 2002, Kluwer Academic Press, Dordrecht, The Netherlands, pp. 65-70, 2003

[7] Boucke, A.: Kopplungswerkzeuge für aeroelastische Simulationen. Dissertation, RWTH Aachen, 2003

[8] Braun, C., Boucke, A., Hanke, M., Karavas, A., Ballmann, J.: Prediction of the Model Deformation of a High Speed Transport Aircraft Type Wing by Direct Aeroelastic Simulation. Krause, Jäger, Resch (Ed.): High Performance Computing in Science and Engineering 03, Springer-Verlag, pp. 331-342, 2003

[9] Kämpchen, M., Dafnis, A., Reimerdes, H.-G., Britten, G., Ballmann, J.: Dynamic Aero-Structural Response of an Elastic Wing Model. Journal of Fluids and Structures, Vol. 18, pp. 63-77, 2003

[10] Kämpchen, M., Dafnis, A., Reimerdes, H.-G.: Aero-Structural Response of a Flexible Swept Wind Tunnel Wing Model in Subsonic Flow. IFASD International Forum on Aeroelasticity and Structural Dynamics, Amsterdam, 2003

[11] Braun, C., Boucke, A., Ballmann, J.: Numerical Prediction of Wing Deformation of a High Speed Transport Aircraft Type Wind Tunnel Model by Direct Aeroelastic Simulation. IFASD 2005, Munich, Germany, paper IF 147

[12] Wigley, D.A. (prep.): ETW Materials Guide. Document ETW/D/95005, Köln 1996

[13] Wagner, J. A.: Mechanical Behavior of 18 Ni 200 Grade Maraging Steel at Cryogenic Temperatures. AIAA-85-0704, 1985

[14] Brakhage, K.-H., Lamby, Ph.: CAGD Tools for High Quality Grid Generation and Sparse Representation. Proceedings of the 8th International Conference on Numerical Grid Generation in Computational Field Simulations, Waikiki Beach, Hawaii. Hrsgb.: B.K. Soni, J.F. Thompson, J. Häuser, P. Eiseman, pp 599-608, 2002

[15] Bartels, R.E., Edwards, J.W.: Cryogenic Tunnel Pressure Measurements on a Supercritical Airfoil for Several Shock Buffet Conditions. NASA TM-110272, 1997

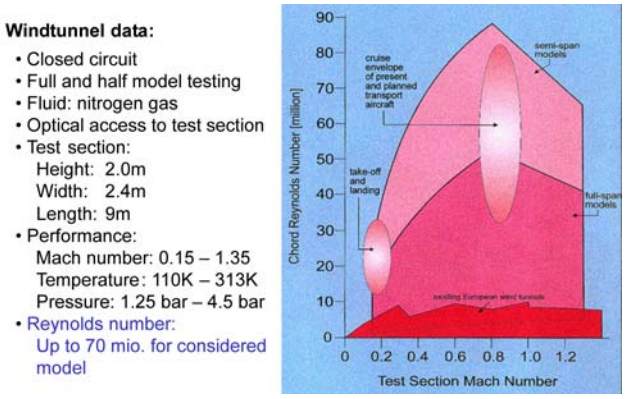

Figure 1: Envelope of the experimental conditions in the European Transonic Windtunnel (ETW) compared with common windtunnels

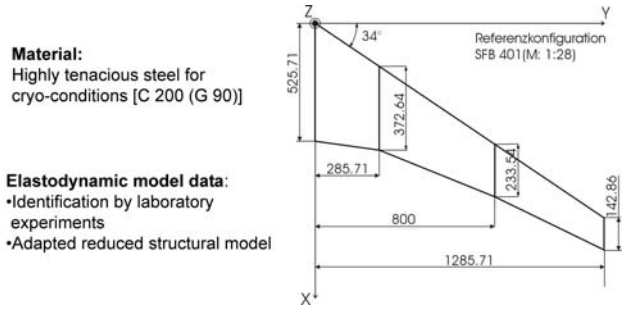

Figure 2: Planview of the 1st design of the Model (1:28 scaled model of 40m half span wing)

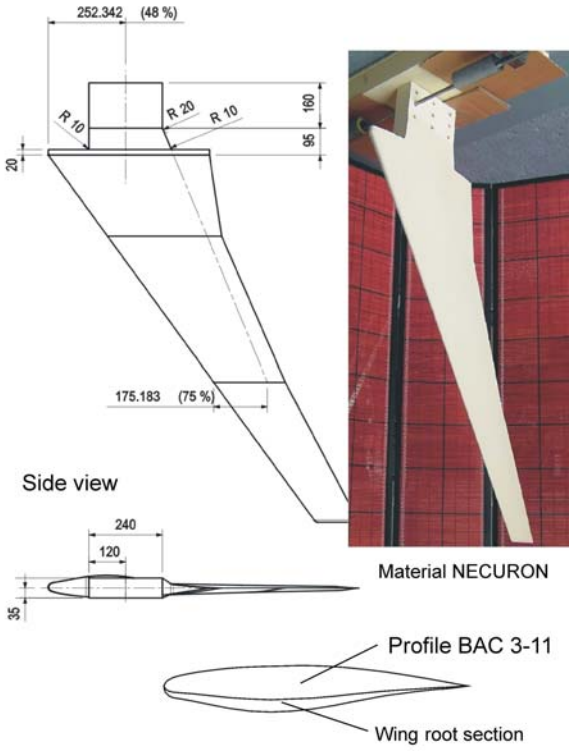

Figure 3: Wing model geometry 1st design and CNC 1:1 manufacturing test in a view model material

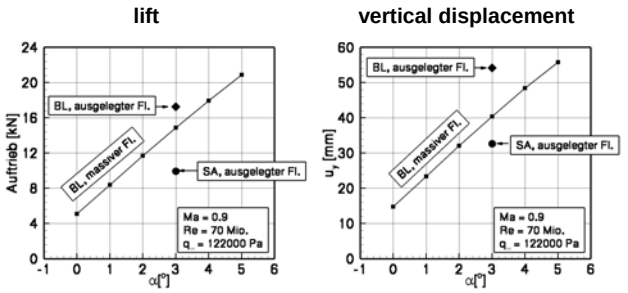

Figure 4: Dimensioning wing model loads and tip displacement for the 1st design

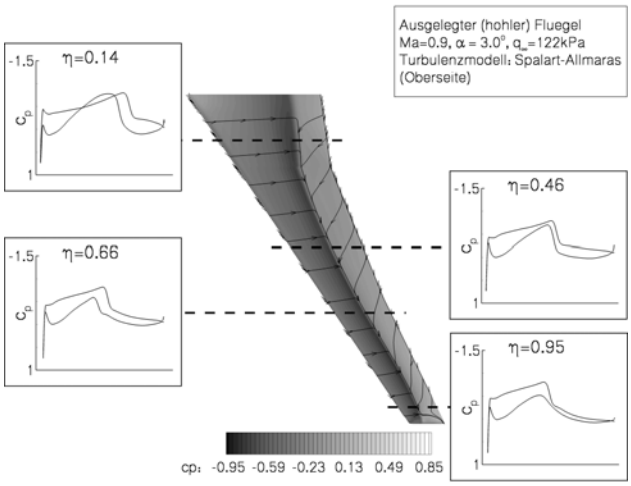

Figure 5: Flow about the static equilibrium configuration of the windtunnel wing model, 1st design

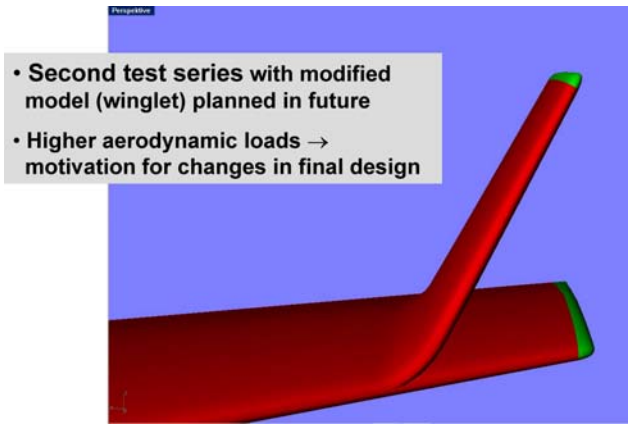

Figure 6: Modification concept for a 2nd test series with a winglet additionally, span unchanged, motivation for enlarged cross-section in the final design of the wing model

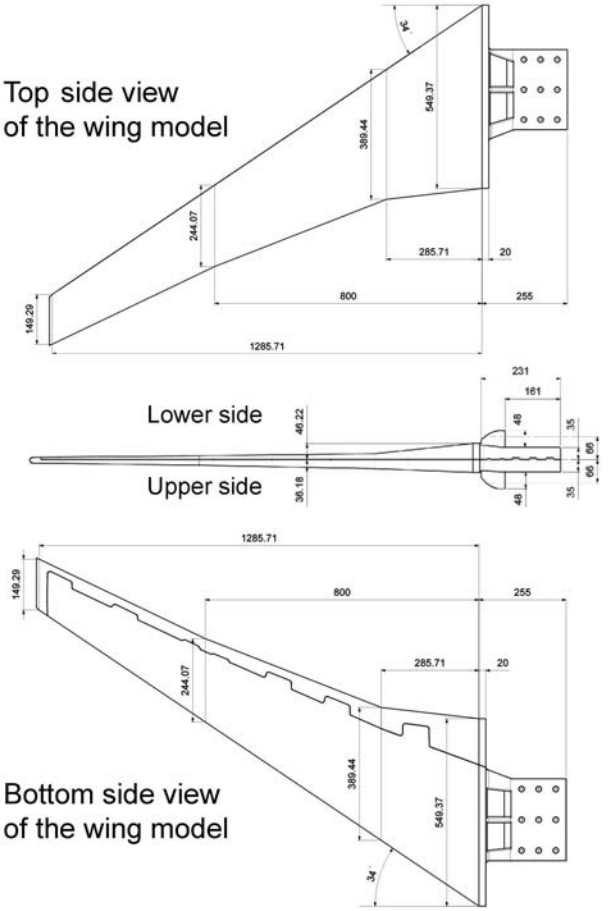

Figure 7: Geometry of the final design of the SFB 401 windtunnel model for experiments in ETW, aerodynamic mean chord amc=0.3445 m

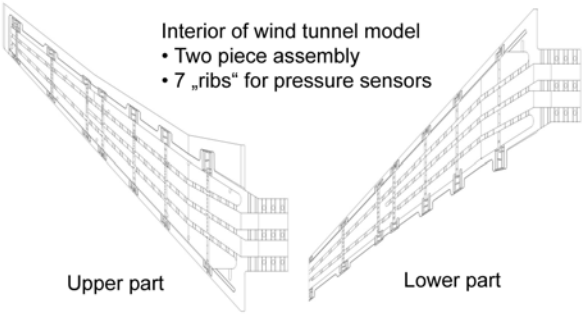

Figure 8: Interior of windtunnel model

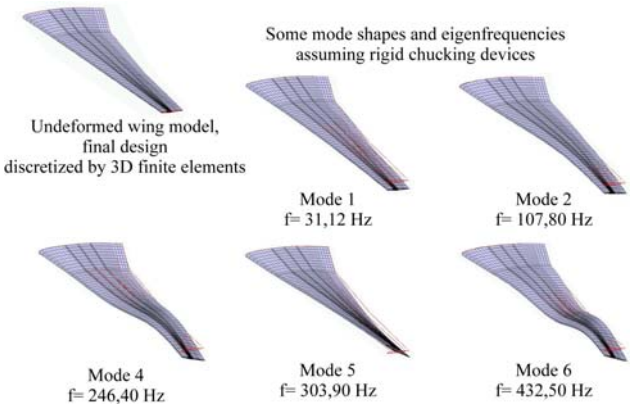

Figure 9: Bending and torsional mode shapes and eigenfrequencies when model is fixed in the root section

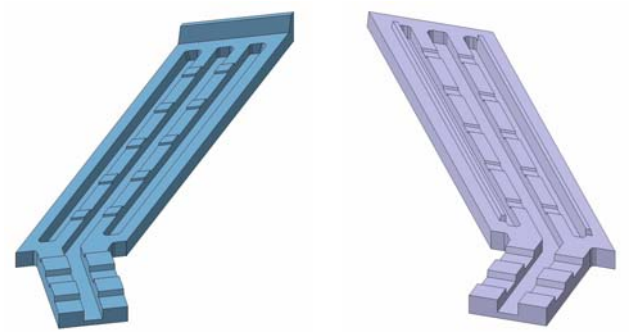

Figure 10: Pre-model for analysis of contact surface design

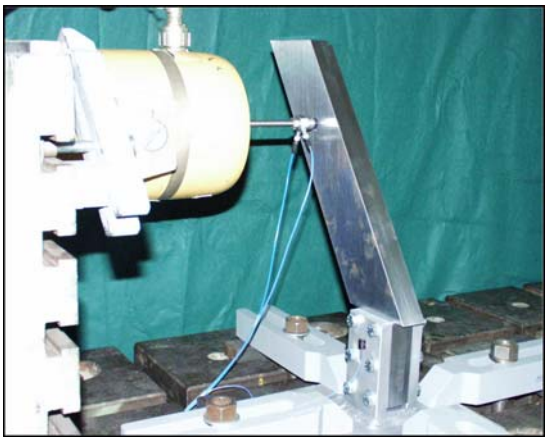

Figure 11: High cycle testing w.r.t. fracture toughness of screws (influence of dry friction / contact phenomena)

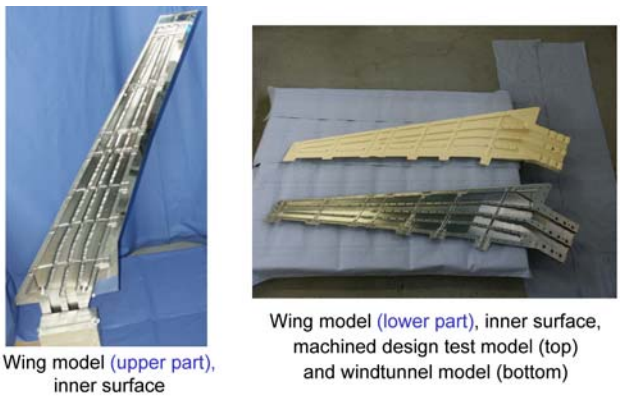

Figure 12: Interior of the manufactured windtunnel model

Figure 13: Photography of the manufactured wing model

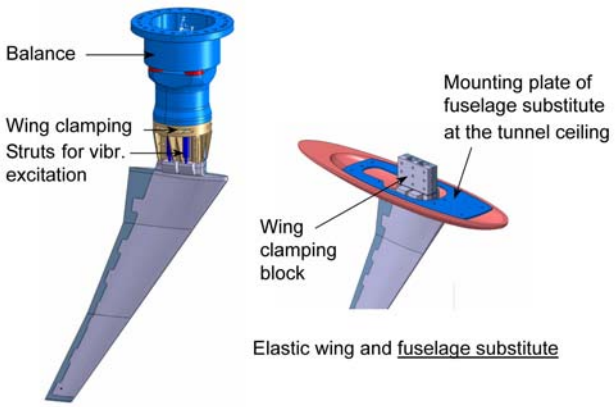

Figure 14: Complete windtunnel assembly. No contact between the elastic wing and the fuselage substitute

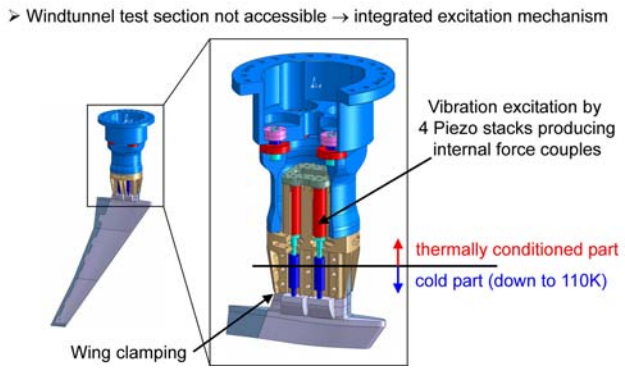

Figure 15: Windtunnel model assembly, balance and excitation mechanism thermally conditioned (heated enclosure)

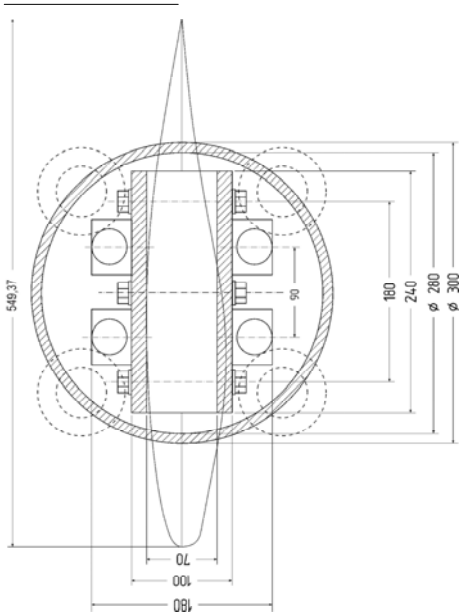

Figure 16: Vibration excitation using 4 piezo-stacks, back-ground 4 elements of piezo balance

Figure 17: Basic excitation test with a pre-model

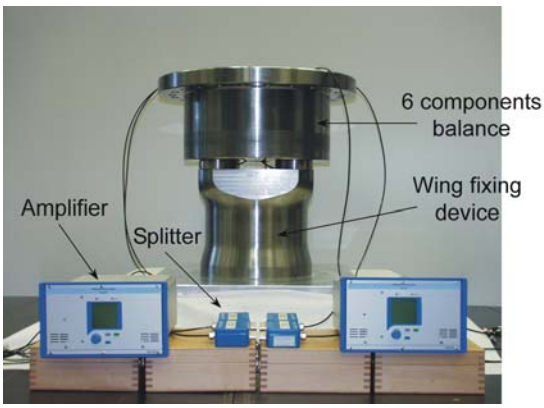

Figure 18: New 6 components piezo balance assembly, completely inside heated enclosure

Technical Details

- 6-component balance
- Four piezo-electric load cells
- Preload force: 300KN
- Measureable forces (depending on preload):

$F_x = \pm 60KN$
$F_y = \pm 60KN$
$F_z = \pm 100KN$

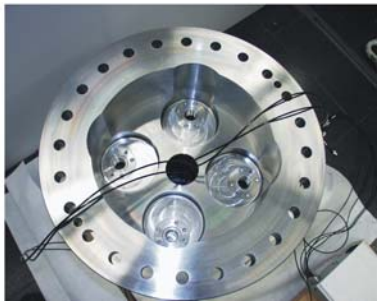

Figure 19: Inside view of the piezo windtunnel balance

Figure 20: Lowest eigenmodes of the piezo balance

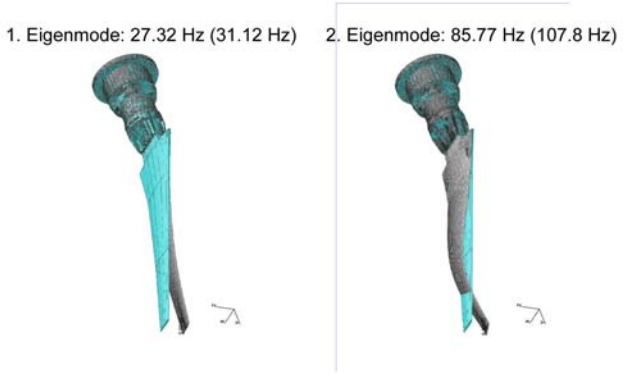

Figure 21: Lowest eigenmodes and frequencies of the complete windtunnel assembly including balance. Values of Fig. 14 in brackets

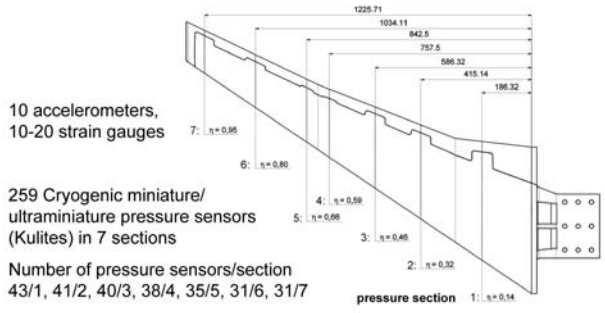

Figure 22: Measuring sensor equipment of the wind-tunnel wing model

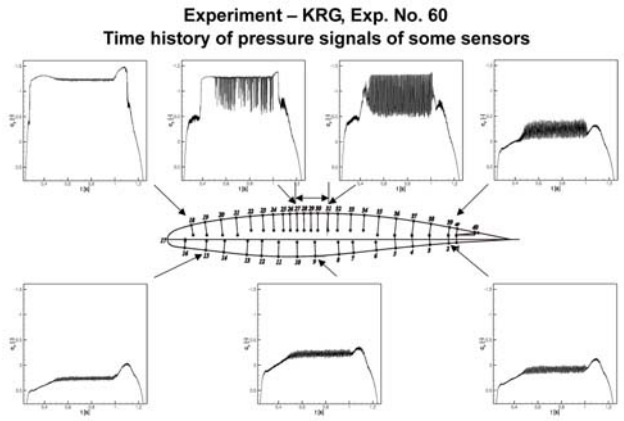

Figure 23: Pressure sensor testing, using a BAC 3-11 airfoil model at lower Reynolds number

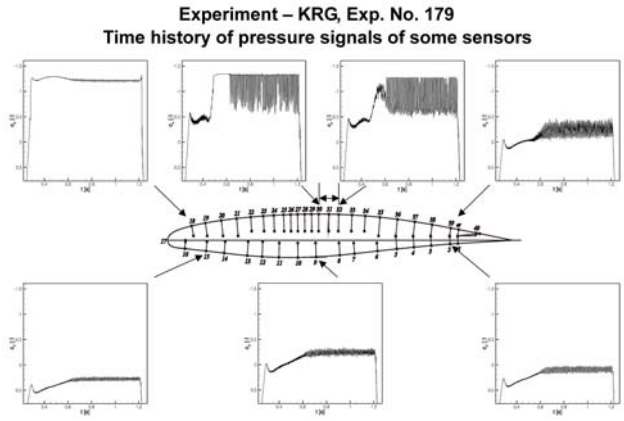

Figure 24: Pressure sensor testing, using a BAC 3-11 airfoil model at higher Reynolds number (realised by cryogenic conditions)

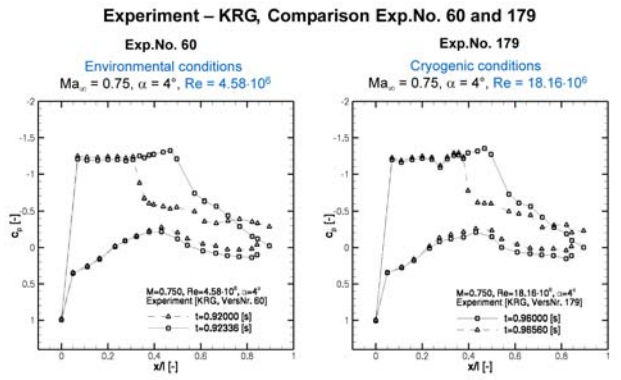

Figure 25: Comparison of the two instantaneous pressure distributions, corresponding to the most upstream and the most downstream shock positions, for two buffet cases with different Reynolds numbers

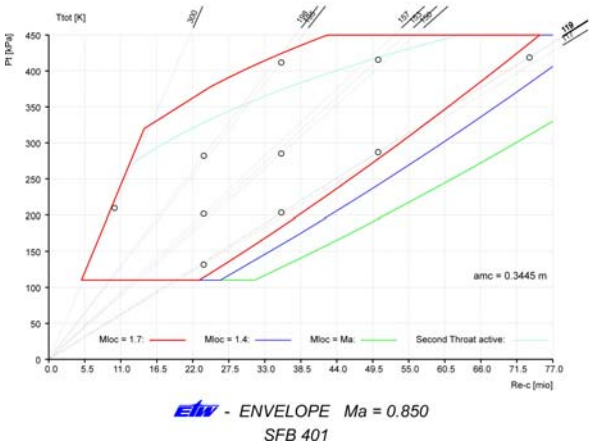

Figure 26: One of three test envelopes for aeroelastic testing of the wing model in ETW, aerodynamic mean chord amc = 0,3445

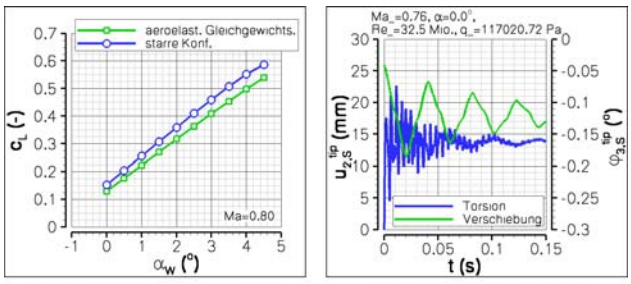

Figure. 27: Preliminary numerical results for the 1st design of the HIRENASD wing model applying a Timoshenko beam model. Left figure: Comparison of lift ignoring deformation (upper curve) and aeroelastic equilibrium deformation (lower curve). Right figure: Wing tip vertical and torsional oscillation decay curves for free vibration simulation